Analog MPPT Comparison for Interplanetary Small Satellites Missions

C. Torres, A. Garrigós, J. M. Blanes, P. Casado, D. Marroquí, C. Orts.

Miguel Hernández University of Elche

Industrial Electronics Group

Elche, Spain

E-Mail: c.torres@umh.es

URL: http://www.umh.es

Acknowledgment

Keywords

Abstract

This paper describes and compares two different Maximum Power Point Tracking (MPPT) techniques devised for micro satellite Solar Array Regulation (SAR). An Analog Global MPPT is introduced and compared with an Analog Oscillating MPPT. Advantages and limitations are discussed. Experimental validation has been carried out using a Power Conditioning Unit and different I/V curves.

Introduction

The use of small satellites with attitude control and ability to perform orbital jumps is nowadays an increasingly widespread practice, which allows interplanetary or deep space missions at a lower cost than traditional space missions with larger spacecrafts. For this reason, an increasing number of companies and scientific research groups are working on the development and evolution of the different subsystems that make them up.
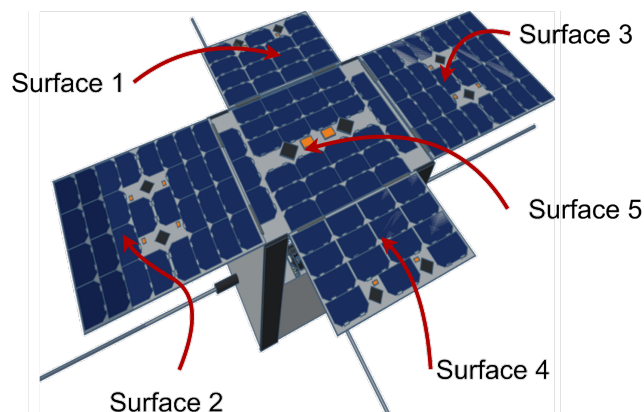

Fig. 1: Rendered image of the proposed solar cell distribution in deployable and body-mounted panels.

In this context, a power subsystem for a deep space mission with a variable distance between 1.5 AU (astronomical unit) and 2 AU from the Sun has been proposed in [1]. That platform has a volume of 36 U, a size of 30 x 30 x 40 cm and a weight around 50 kg including fuel and payload. To power the various subsystems the satellite has a total amount of 120 solar cells model 3G30C from the manufacturer Azur Space distributed in six solar arrays (SA). Each SA is distributed in two parallel connected strings made up of ten series-connected solar cells. The solar cells are accommodated in four deployable panels plus a body-mounted panel, as represented in Fig. 1.

The Power Conditioning Unit (PCU) is responsible for extracting power from the six SAs, charge the batteries and supply the rest of subsystems. The main element of the PCU is the Solar Array Regulator (SAR), which in this case, is divided into six independent phases with their outputs connected in parallel, see Fig. 2. Each phase includes a synchronous Buck converter powered by one of the six available SA's, an error amplifier that regulates the end of charge battery voltage or extracts maximum power from the photovoltaic source otherwise. A detailed explanation of the SAR control loop operation is described in [2]. Additionally, as a means of protection, the SAR has three overvoltage monitors that disconnect the Buck converters from the SA's if the battery voltage exceeds a pre-set threshold. The SAR has been designed following European Space Agency (ESA) guidelines to assure single point failure free (SPFF) operation
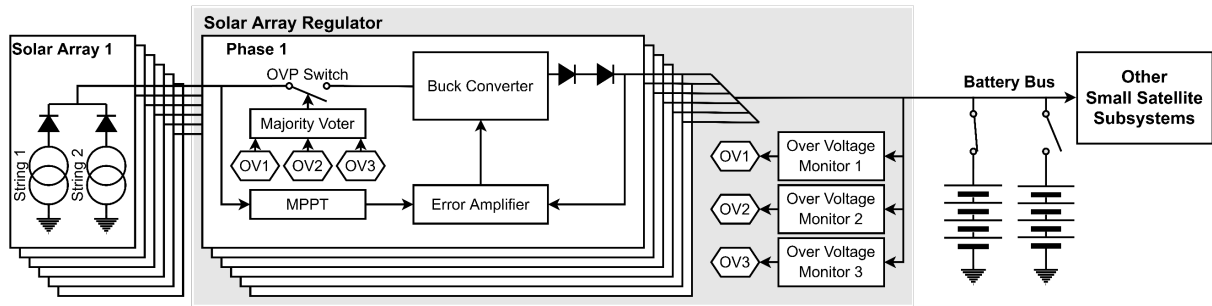

Fig. 2: Block diagram of the proposed PCU.

In extreme operating conditions, such in interplanetary missions, it is expected to have very different solar cell I/V curves in the same solar array. This may be due to different factors, some of them are summarised in Table I.

Table I: Effects causing mismatches between various solar cells.

Factor	*Causes and effects*
Δ Irradiance	Variations in irradiance affect the amount of current supplied by each solar cell. Further, the arrangement of the solar cells on different facets of the satellite can cause them not to receive irradiance homogeneously or to be affected by the shadow of some other element. This effect can be aggravated if the deployment of the panels is not fully successful.
Δ Temperature	Variations in temperature will affect the voltage and current provided by the solar cells. Temperature variations may be due, for example, to the location of the cell on the satellite. In the proposed satellite, cells located on the body-mounted panel could experience higher temperature than cells located on the rest of the facets of the satellite.
Cell Mismatch	Due to the manufacturing process, solar cells may present variations of up 10% in current and open circuit voltage V_{OC}.
Aging	Aging, mainly due to operation in highly radiation environments, produces a degradation in both voltage and current. Aging is independent in each cell.
Micrometeorites	Impacts produced by micrometeorites can damage the cells producing different degradation effects.

The aforementioned factors can create complex P/V curves such as those shown in Fig. 3. Fig 3 shows simulated I/V and P/V curves of a single SA at 1.5 AU with different degradation effects.

As can be seen, degradation, shadowing and other effects create P/V curves with several local maximum power points (MPP). This can cause that some oscillation-based Maximum Power Point Trackers (MPPTs) to get trapped oscillating around a local maximum, making impossible to extract the maximum available power from the solar panel.
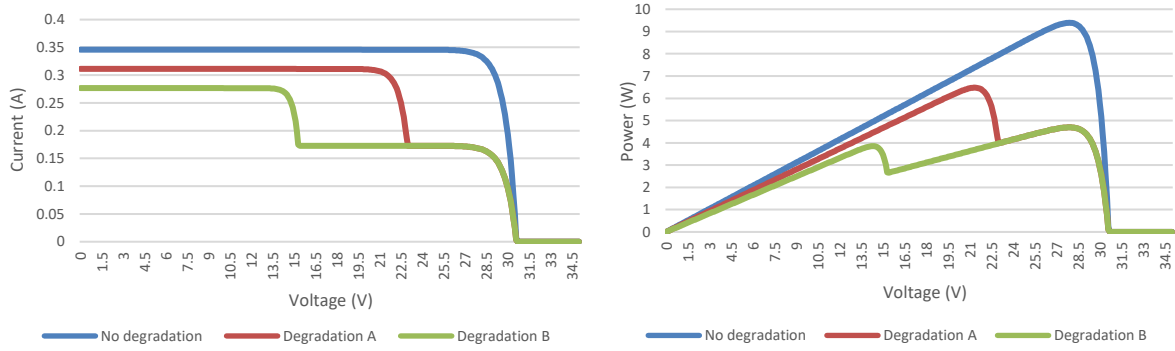

Fig. 3: Representation of curves of SA in different conditions. On the left I/V curve. On the right P/V curve.

In this work, the design of an analog oscillation-based MPPT and an Analog Global MPPT (AGMPPT) are presented. Both designs are compared, and their performance is measured under different I/V curves scenarios. Finally, the results obtained are discussed and the conclusions are presented.

Analog oscillation-based MPPT

The first of the two methods proposed in this work is an oscillating MPPT. This method, first proposed in 1960s [3], has been adapted and widely adopted in many space missions due to its simplicity and robustness [4]. This MPPT requires measurement of SA voltage and current. Fig. 4 shows the diagram of the proposed MPPT.
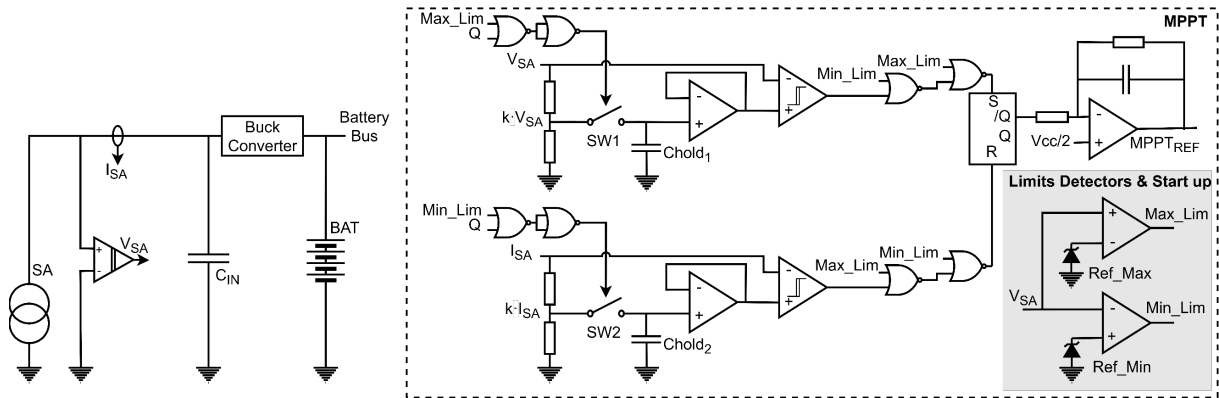

Fig. 4: Diagram of the proposed SAR using the oscillating-based MPPT method.

Initially, the MPPT starts at OC (open circuit) of the SA. In this moment, the output voltage of the SA is captured and the MPPT reference decreases causing an increase in the duty cycle of the DC-DC converter. As the duty cycle of the dc-dc converter increases the SA operating point moves towards to SC (short circuit), until the voltage V_{SA} decrease a certain (ΔV) amount determined by $k \cdot V_{SA}$. At that moment, RS flip-flop's SET signal becomes active, output Q changes its state and I_{SA} is recorded. As a result, the MPPT reference increases, the duty cycle of the converter is reduced, and the input voltage

moves towards OC until I_{SA} decrease a certain (ΔI) amount determined by $k \cdot I_{SA}$. Then, RS flip-flop's RESET signal turns on, the MPPT reference is inverted, and the cycle starts again. This process is repeated continuously, causing the MPPT to oscillate around the Maximum Power Point (MPP) of the SA, as explained in detail in [3] and [4]. The MPPT reference signal is generated by integrating the flip-flop's output signal. Additionally, the MPPT has maximum and minimum voltage limit detectors, that forces the MPPT to work within a defined voltage range and ensure system starts.

Analog Global MPPT

The second method analysed is an Analog Global MPPT. The block diagram of the proposed AGMPPT is shown in Fig. 5. The AGMPPT uses the input capacitor of the Buck converter to scan the solar array and to save the global MPP (GMPP). The operation principle is as follows, first, the buck converter is turned-off and the input capacitor discharged (CLK1 signal). Once CLK1 is released, the I/V curve is scanned as the capacitor charges. During I/V curve scanning, the AGMPPT detects the global MPP using a peak detector. To measure the power (P), an analog PWM multiplier computes $I_{SA} \cdot V_{SA}$. The V_{SA} voltage corresponding to the global MPP of the SA is stored to be used later as a reference for the Buck converter during MPPT period. Once the scan is complete, the Buck converter is turned-on again. The converter remains on and working in the global MPP during the MPPT *on*-period. When the *on*-period (MPPT period) ends, the input capacitor is discharged again and the scanning process is repeated, thus obtaining a new global MPP for the buck converter. A more detailed explanation of the operating principle of this AGMPPT is provided in [5].
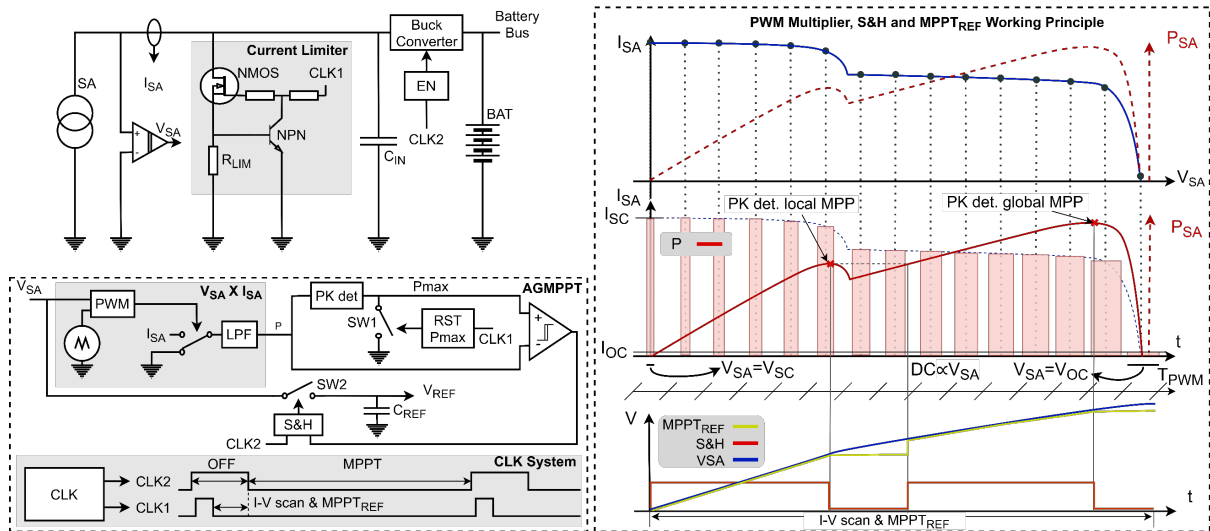

Fig. 5: Diagram of the proposed SAR using the AGMPPT method.

Theoretical comparison of the oscillating-MPPT vs the AGMPPT

Oscillating, perturb and observe and other MPPT techniques have been widely used due to its high efficiency and good performance. However, all of them have a major drawback, they cannot discriminate between local and global MPP. This can be a serious problem in certain I/V curves, as could be the case of the curve "Degradation A" shown in Fig. 3. In that case, the MPPT starts working from V_{OC} and move towards the I_{SC} point on the I/V curve, getting trapped oscillating around a local MPP.

The AGMPPT has been proposed to overcome this issue, since the full I/V curve is scanned. This AGMPPT requires a scan time during which the converter remains off, affecting its average efficiency. To minimize this issue, a compromise between the *off* time (t_{OFF}) and the MPPT-*on* time (t_{ON}) must be reached. The AGMPPT period (T) is equal to $t_{OFF} + t_{ON}$.

Another critical aspect that must be taken into consideration is the implementation of the analog multiplier. Simple and low consumption device is required to maximise efficiency, but also accuracy and fast response is essential, otherwise it is not possible to perform a correct scan of the I/V curve and, consequently, an erroneous MPP point would be used. Since monolithic space-qualified analog multipliers are scarce and complex, a simple analog PWM multiplier is used.

Regarding the implementation of both MPPT, Table II indicates the number of components, classified by groups, that are required for the implementation of each of the designs. It is observed that the number of components is similar in both MPPTs, so it is assumed that the area required for the implementation is also similar. As a main difference in terms of components is that oscillating-MPPT does not require any timer (i. e. 555 IC), although, it uses two more comparators than the AGMPPT. Therefore, the implementation cost of both systems is similar.

Table II: Comparison of the number of components required in each implementation.

Component	Nº of components		Component	Nº of components		Component	Nº of components	
	Osc. MPPT	AGMPPT		Osc. MPPT	AGMPPT		Osc. MPPT	AGMPPT
Resistors	27	33	Comparators	4	2	555 IC	0	2
Capacitors	23	25	Diodes/Zener	3	2	OpAmp	4	4
Logic gates	8	9	Switches	2	3	I sensor	1	1
BJT Trans.	0	2	Flip-flops	1	0	MOSFET	0	2
Total nº of MPPT components:	**73**				**Total nº of AGMPPT components:**		**85**	

Implementation of both MPPTs and experimental tests

To verify that both MPPTs behave as expected, the complete SAR is implemented with the oscillating-MPPT integrated, and the AGMPPT implemented on a separate PCB. To optimize the period (T) of the AGMPPT, several experimental efficiency measurements have been carried out, obtaining a maximum efficiency for T = 2 s and t_{Off} = 45 ms. The developed prototypes are shown in Fig. 6.
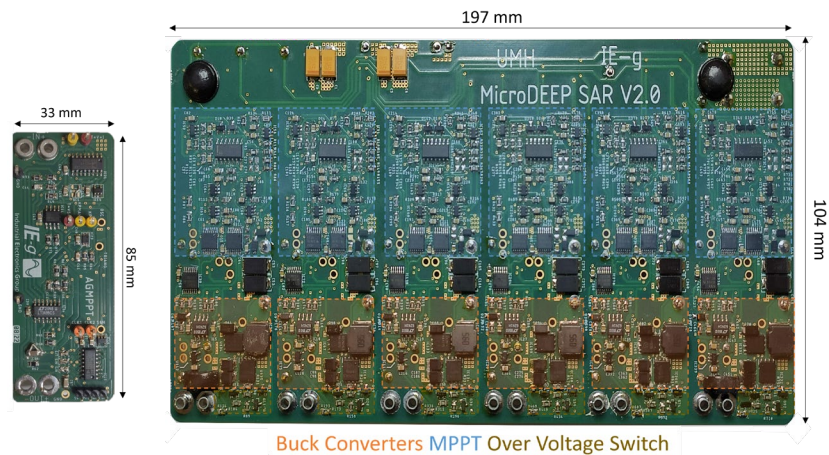

Fig. 6: AGMPPT is shown on the left. Full SAR with MPPT is shown on the right.

Tests have been performed using two different scenarios corresponding to a solar array in configuration 10S2P at a sun distance of 1.5 AU (610w/m^2, -30 ºC) and 2 AU (342 w/m^2, -54,3 ºC) respectively. For each scenario, three I/V curves are considered. First curve considers an ideal I/V curve with a single MPP. Second (Degradation 1) and third (Degradation 2) cases consider I/V curves with two local MPPs. These curves are simulated using two Agilent E4351B SA simulators connected in parallel. The curves, as well as the working point set by each MPPT in each of the tests, are shown in Fig. 7.
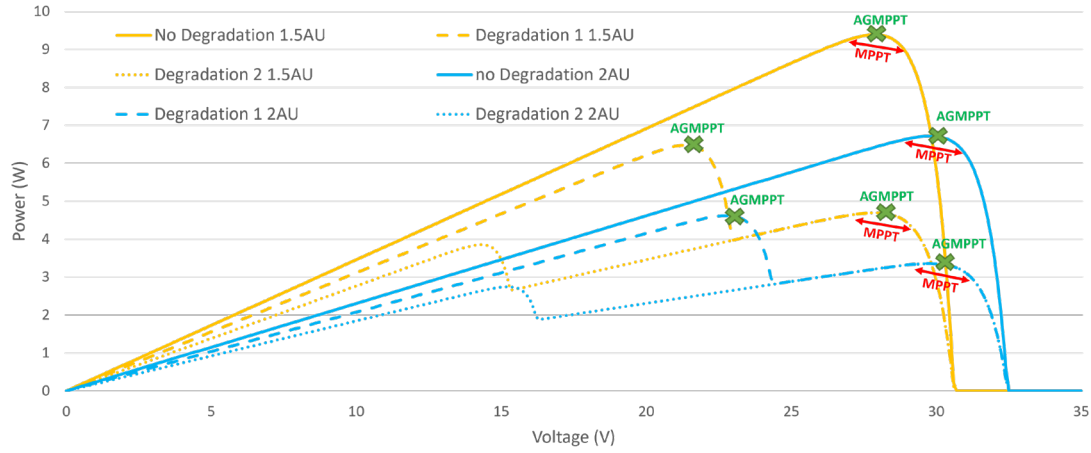
Fig. 7: Different simulated curves and working points obtained by both MPPT

To carry out the tests, an ITECH IT-M3412 battery simulator connected to the SAR output has been used. All tests have been carried out at a fixed output voltage of 16V. Measurement equipment is the following: Tektronix MDO3104 oscilloscope, Tektronix TPP1000 voltage probes and Tektronix TCPA0030A current probes. Efficiency measurements is performed by calculating the average power extracted from the SA divided by the total power available in the SA at MPP.

The results show that the oscillating-MPPT works correctly when the global MPP is the closest to the V_{OC} point. These are the "No Degradation" and "Degradation 2" cases for curves located both 1.5 AU and 2 AU. In cases where there is a local MPP between the global MPP and the V_{OC} point, it is observed that the oscillating MPPT is trapped working in that local MPP. That is the case "Degradation 1" at both 1.5 AU and 2 AU.

On the other hand, the AGMPPT scans properly the entire SA I/V curve, being able to identify its global MPP and working on it in all cases. Next figures show the behaviour of each of the MPPTs for some of the tested curves.

Fig. 8 shows the operation of the oscillating-MPPT with "Degradation 1" curve at a sun distance of 1.5 AU. Initially the MPPT starts at the V_{OC} point, as shown by the V_{SA} signal. The MPPT takes about 0.5s to start up because the control loop is slow and is initially saturated. Once steady-state is achieved, it oscillates around the 28 V point on the I/V curve, which, as shown in Fig. 7, corresponds to the voltage around the local MPP of SA. From this moment on, the MPPT is permanently working around the local MPP, thus wasting part of the power of the SA. Additionally, Fig. 8 also shows the VSA voltage, the ISA current, the power extracted from the SA and the MPPT reference signal.
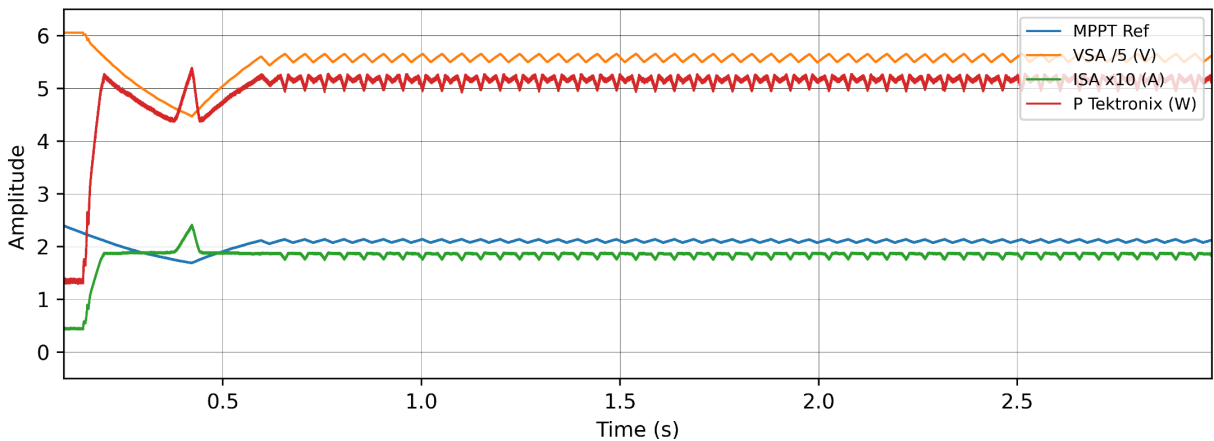

Fig. 8: "Degradation 1" curve, distance from sun of 1.5 AU. oscillating-MPPT.

On the other hand, Fig. 9 shows the behaviour of the AGMPPT in these same operating conditions and P/V curve. Between t = 0 and t = 0.046s, the capacitor is discharged, and the I/V curve is scanned. It is observed that power measured in the AGMPPT multiplier (P AGMPPT) corresponds accurately to the power measured in the oscilloscope (P Tektronix). It can be also observed that peak power detector identifies the global MPP of the I/V curve and stores the V_{SA} voltage value, which is used later as a reference for the Buck converter. At t = 0.046s, the Buck converter turns on and works in the global MPP, taking the previously stored value as a reference. The converter remains working at the global MPP for the next 2 seconds. Then, it will turn off again to repeat the scanning process. It should be noted that the AGMPPT has been able to work at the global MPP of the P/V curve, obtaining an efficiency greater than 96%, while the oscillating one has been stuck at the local MPP, reducing its efficiency to 75%.
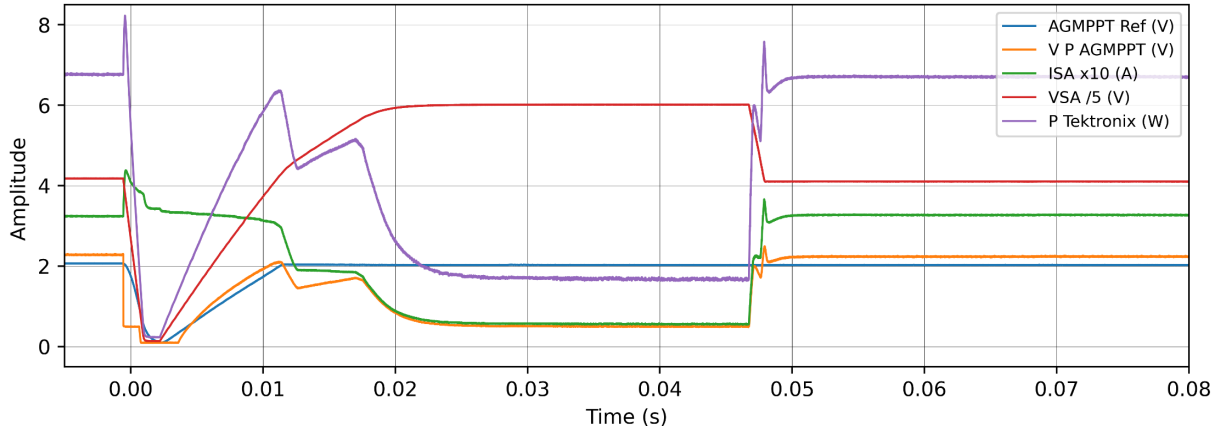

Fig. 9: "Degradation 1" curve, distance from sun of 1.5 AU. AGMPPT.

A second batch of measurements consider the 1.5AU, "Degradation 2" I/V curves. Fig. 10 shows the result obtained with the oscillating-MPPT. The MPPT starts at the V_{OC} point of the SA I/V curve. Once the system has started, the operating point moves to the next maximum found when tracking the I/V curve from the V_{OC} point to the I_{SC} point. In this case, that local maximum found corresponds to the global MPP, so now the oscillating-MPPT operates in the global MPP. The V_{SA} and I_{SA} signals show how the MPPT is oscillating around the MPP. Additionally, the power extracted from the SA (P Tektronix) and the MPPT reference signal (MPPT Ref) are shown. It should be noted that in this case the efficiency is better than 99%.
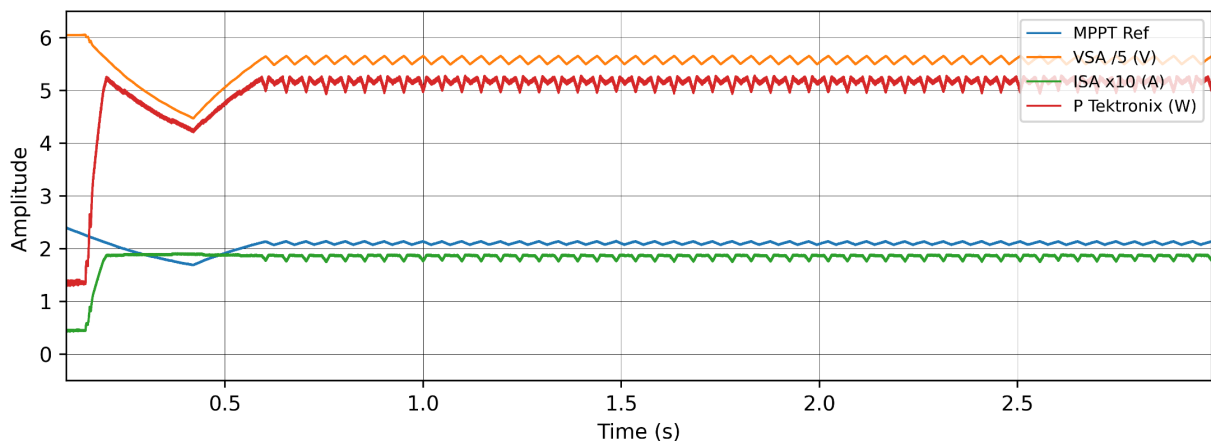

Fig. 10: "Degradation 2" curve, distance from sun of 1.5 AU. oscillating-MPPT.

The last test has been carried out using the AGMPPT with the previous I/V curve. The results obtained are shown in Fig. 11. It is shown that AGMPPT scans the I/V curve accurately, retaining at each moment the voltage V_{SA} corresponding to the MPP of the section of the curve already scanned. Once the scanning

process is finished, the Buck converter is activated, setting the I/V point of the curve corresponding to the detected global MPP as its working point. The converter will remain working in the global MPP for 2 seconds. Then, the scanning process will start again. It should be noted that the efficiency obtained by the AGMPPT in this case is better than 97.60%, being slightly below the efficiency obtained with the oscillating MPPT under these same conditions.
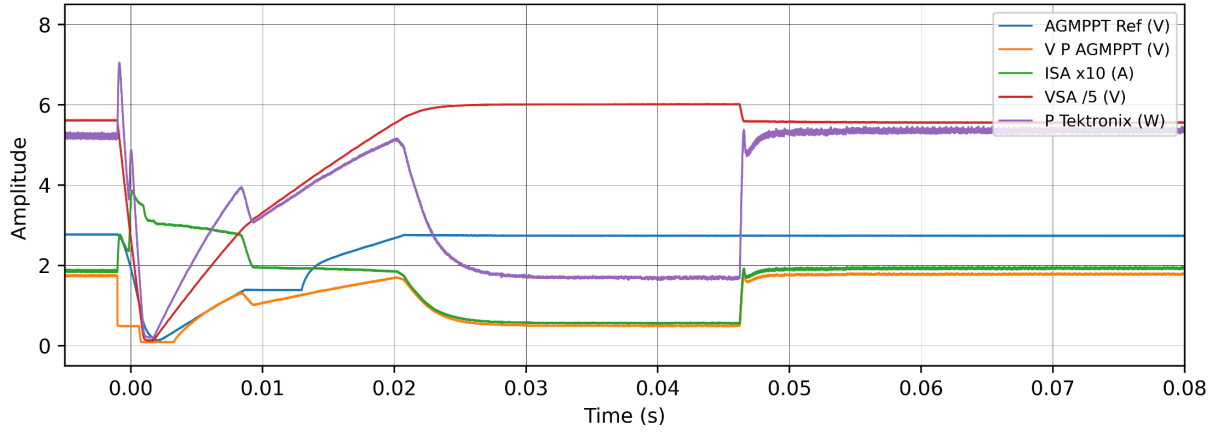

Fig. 11: "Degradation 2" curve, distance from sun of 1.5 AU. AGMPPT.

Experimental validation continues repeating these tests for the different curves, obtaining similar results. The following section shows the efficiency results obtained in each test.

Results

The data related to the efficiency of the MPPTs obtained experimentally in the various tests are shown in Table III. It is observed that when the curves do not have local MPP, both MPPTs work correctly, obtaining efficiencies between 96.01% and 98.82%. It is observed that in this case the efficiency of the oscillating-MPPT is slightly better than that of the AGMPPT. In the cases in which the curves present local MPP, but these are not between the global MPPT and the V_{OC} point (Degradation 2), the results are similar. The oscillating-MPPT has obtained a maximum efficiency of 99.06% while the AGMPPT has obtained a maximum efficiency of 97.65%.

On the other hand, in the cases in which the SA I/V curve presented local MPP between the global MPP and the V_{OC} point (Degradation 1), it is observed that the efficiency of the AGMPPT has remained between 96.02% and 96.07%. However, the efficiency obtained by the oscillating-MPPT has decreased to values between 71.90% and 75.04%. It is in this type of curves where the AGMPPT shows a much better performance than the oscillating-MPPT.

Table III: Experimental results obtained.

	SA MPP Power (W)		*Average Power Output (W)*				*Efficiency (%)*			
			AGMPPT		*Osc. MPPT*		*AGMPPT*		*Osc. MPPT*	
Sun Distance (AU):	*1.5*	*2.0*	*1.5*	*2.0*	*1.5*	*2.0*	*1.5*	*2.0*	*1.5*	*2.0*
No Degradation	9.684	6.76	9.36	6.49	9.564	6.68	96.65	96.01	98.76	98.81
Degradation 1	6.45	4.63	6.1936	4.448	4.84	3.329	96.03	96.07	75.04	71.90
Degradation 2	4.92	3.4	4.773	3.32	4.829	3.368	97.01	97.65	98.15	99.06

In general, both MPPTs have worked correctly, although the oscillating-MPPT has obtained a slightly higher efficiency than the AGMPPT in most cases. However, in some curves the oscillating-MPPT has presented efficiency losses of almost 30%, while the AGMPPT has always remained above 96%.

Analysing these results and considering that the cost of implementation and the area required by both models is very similar, it can be concluded that the use of the AGMPPT is advantageous compared to the use of the oscillating-MPPT in applications in which complex P/V are expected and SA power optimization is critical. This is because the AGMPPT ensures high performance with any kind of I/V curve with a penalty of 1% of efficiency reduction compared to traditional methods. If complex I/V curves are not anticipated, oscillating-MPPT might be more indicated.

Conclusion

In this work, two MPPT analog methods have been presented, an oscillating-MPPT and an AGMPPT, for high performance small satellites. The application to which both MPPTs are intended has been presented, the electrical diagrams have been shown and the operating principle of both has been explained. Subsequently, a theoretical comparison is made. This comparison presents the main advantages of each design, as well as the bill of materials that allows a fair estimation of the area and the cost of implementing one design compared to the other. Then, both designs have been implemented and tests have been carried out under various conditions with the aim of validating the correct operation of the designs. The results of the tests show that both MPPTs behave as expected. Oscillating-MPPT performs slightly better than AGMPPT if the I/V curve does not present local MPP between the global MPP and the V_{OC}. However, it cannot operate properly if the first MPP found is a local MPP. On the other hand, the AGMPPT has high efficiency in all cases, which makes it ideal for use in applications where reliability is a critical design aspect and high performance is sought.

References

[1]   J. A. Carrasco *et al.*, "Micro-platform Power System for Scientific Deep Space Exploration," in *12th European Space Power Conference*, 2019.

[2]   A. Garrigós, J. L. Lizan, J. M. Blanes, and R. Gutierrez, "Exploring the Use of the LT3480 (RH3480) Circuit as Low-Power, Low-Voltage Solar Array Regulator," in *10th European Space Power Conference*, 2014, ESA SP-719.

[3]   A. F. Boehringer, "Self-Adapting dc Converter for Solar Spacecraft Power Supply," *IEEE Trans. Aerosp. Electron. Syst.*, vol. AES-4, no. 1, pp. 102–111, 1968, doi: 10.1109/TAES.1968.5408938.

[4]   W. Denzinger, "Electrical power system of globalstar," *Proc. 4th Eur. Sp. Power Conf.*, pp. 171–174, 1995.

[5]   A. Garrigós, D. Marroquí, J. M. Blanes, R. Gutiérrez, M. Compadre, and C. Clark, "An analog global maximum power point tracking for photovoltaic systems: Application to nanospacecrafts," *2017 19th Eur. Conf. Power Electron. Appl. EPE 2017 ECCE Eur.*, vol. 2017-Janua, pp. 1–9, 2017, doi: 10.23919/EPE17ECCEEurope.2017.8098986.